THE JOURNAL OF BIOLOGICAL CHEMISTRY
Vol. 272, No. 7, Issue of February 14, pp. 4261–4268, 1997
© 1997 by The American Society for Biochemistry and Molecular Biology, Inc.
Printed in U.S.A.

Three-dimensional Structure of Myelin Basic Protein

I. RECONSTRUCTION VIA ANGULAR RECONSTITUTION OF RANDOMLY ORIENTED SINGLE PARTICLES*

(Received for publication, September 19, 1996)

Daniel R. Beniac‡, Maria D. Luckevich‡, Gregory J. Czarnota§, Thomas A. Tompkins‡¶‖, Ross A. Ridsdale‡, F. Peter Ottensmeyer§, Mario A. Moscarello¶, and George Harauz‡**

From the ‡Department of Molecular Biology and Genetics, University of Guelph, Guelph, Ontario N1G 2W1, Canada, §Department of Molecular and Structural Biology, Ontario Cancer Institute, 610 University Avenue, Toronto, Ontario M5G 2M9, Canada, and ¶Department of Biochemistry Research, Hospital for Sick Children, 555 University Avenue, Toronto, Ontario M5G 1X8, Canada

Myelin basic protein (MBP) plays an integral role in the structure and function of the myelin sheath. In humans and cattle, an 18.5-kDa isoform of MBP predominates and exists as a multitude of charge isomers resulting from extensive and varied post-translational modifications. We have purified the least modified isomer (named C1) of the 18.5-kDa isoform of MBP from fresh bovine brain and imaged this protein as negatively stained single particles adsorbed to a lipid monolayer. Under these conditions, MBP/C1 presented diverse projections whose relative orientations were determined using an iterative quaternion-assisted angular reconstitution scheme. In different buffers, one with a low salt and the other with a high salt concentration, the conformation of the protein was slightly different. In low salt buffer, the three-dimensional reconstruction, solved to a resolution of 4 nm, had an overall "C" shape of outer radius 5.5 nm, inner radius 3 nm, overall circumference 15 nm, and height 4.7 nm. The three-dimensional reconstruction of the protein in high salt buffer, solved to a resolution of 2.8 nm, was essentially the same in terms of overall dimensions but had a somewhat more compact architecture. These results are the first structures achieved directly for this unusual macromolecule, which plays a key role in the development of multiple sclerosis.

The myelin sheath is a multilamellar membranous structure that surrounds the axons of the central and peripheral nervous systems (1–3). Proteins constitute 30% of the dry weight of central nervous system myelin, with the major ones being proteolipid protein (or lipophilin; 50% of total protein) and myelin basic protein (MBP;[1] 20% of total protein) (1–5). Myelin basic protein-lipid interaction has been shown to be critical for the formation and stability of the multilamellar myelin sheath (6–8), although the physicochemical mechanisms by which this occurs are still not clearly defined despite many investigations (*e.g.* Refs. 9–28). Myelin basic protein was the first agent in brain or spinal cord homogenates discovered to be responsible for experimental allergic encephalomyelitis, which is considered to be an animal model for the human disease multiple sclerosis (29–31).

In all species studied, MBP exists in a number of isoforms as a result of differential splicing of its primary mRNA transcript (32–34). The 18.5-kDa isoform is the most common in mammals, including humans and cattle. The amino acid sequences of the 18.5-kDa isoforms of human and bovine MBP were reported independently by Carnegie *et al.* (29) and by Eylar *et al.* (30), respectively. Briefly, MBP contains (i) no cysteinyl residues, (ii) 12 lysyl and 19 arginyl residues giving it a highly basic character (pI ~10.6), (iii) 11 prolyl residues (including a triproline repeat adjacent to human Thr^{98} and bovine Thr^{97}), (iv) a mitogen-activated protein kinase site (35), and (v) a large number of seryl and threonyl residues making it an excellent substrate for several other protein kinases (36–38). Phosphorylation as well as other extensive post-translational modifications of MBP (*e.g.* GTP binding, ADP-ribosylation, deimination of arginyl residues to citrullinyl residues) create a high degree of microheterogeneity (4, 39–43). The resultant charge isomers of MBP can be separated on a cation exchange column at high pH (40). Component C1 is the least modified and most basic component, and C8 is the most modified. MBP isolated from victims of multiple sclerosis has been shown to be considerably less cationic than that from normal, age-matched controls due to a decrease in the most cationic form (C1) and a consequent relative increase in the less cationic isomers, particularly C8 (43–45). We focus here on the structure of C1 of the 18.5-kDa form of bovine MBP, and in this paper we shall consider "MBP/C1" as meaning this isoform and isomer.

Myelin has been generally considered to be an inert structure, facilitating saltatory conduction of nerve impulses. Thus, the role of MBP has long been assigned to be simply the compaction at the *cytoplasmic* surface of oligodendrocytes or Schwann cells, which eventually becomes the *major dense line* (1–3, 8, 22, 46). However, with the identification of citrulline-containing MBP (42), its implication in demyelination in multiple sclerosis (43–45), and its localization to the *intraperiod line* of myelin (47, 48), it appeared that a division of labor was operative for the plethora of post-translationally modified MBP molecules (4, 43). Other functions of MBP charge isomers include stimulation of phospholipase C activity (49, 50), actin polymerization in conjunction with Ca^{2+}-calmodulin (12, 51), tubulin stabilization (52), or even potential regulatory roles as transcription factors (8). Presently, MBP is generally believed to be the agent responsible for the autoimmune response that precipitates the active degradation of the myelin sheath in multiple sclerosis (*e.g.* Refs. 53 and 54).

* This work was supported by the Multiple Sclerosis Society of Canada (operating grant to G. H.). The costs of publication of this article were defrayed in part by the payment of page charges. This article must therefore be hereby marked "*advertisement*" in accordance with 18 U.S.C. Section 1734 solely to indicate this fact.

‖ Present address: Lallemand Inc., Laboratoire R & D, 6100 Royalmount, Montréal, Québec H4P 2R2, Canada.

** To whom correspondence should be addressed. Tel.: 519-824-4120 (ext. 2535); Fax: 519-837-2075; E-mail: gharauz@uoguelph.ca.

[1] The abbreviations used are: MBP, myelin basic protein; CAPS, 3-(cyclohexylamino)propanesulfonic acid; TEM, transmission electron microscopy; G_{M1}, ceramide-*N*-tetrose-*N*-acetylneuraminic acid where *N*-tetrose is galactose ($1 \xrightarrow{\beta} 3$)-*N*-acetylgalactosamine ($1 \xrightarrow{\beta} 4$)-galactose ($1 \xrightarrow{\beta} 4$)-*N*-acetylneuraminic acid.

Knowledge of the tertiary structure of MBP and its association with lipids and other proteins within the compacted myelin multilayers would facilitate a greater understanding of how it carries out its diverse functions. It is known by spectroscopic studies that MBP probably has a disordered conformation in its isolated form in aqueous solution (5, 55–59) and that its secondary structure changes after phosphorylation or in the presence of lipids or detergents (5, 36, 37, 60–64). The protein interacts strongly with itself and with other proteins (5, 65–71), and sequesters zinc (72), a divalent cation essential for the stability of myelin (73). The structures of small subsegments of MBP have been probed by nuclear magnetic resonance (63, 74–78) or predicted by computational sequence analyses (25, 79–84). However, all attempts to obtain three-dimensional crystals of MBP suitable for x-ray diffractometry (very many have been pursued over the past 2 decades) have failed (85). In this and the accompanying manuscript (86), we describe electron microscopical visualization and molecular modeling studies of MBP. Here, we exploited the well defined images of randomly oriented particles of bovine MBP formed on lipid monolayers formed on the air-water interface to obtain a structure to 2.8-nm resolution via "single particle electron crystallography" (87, 88). A molecular model of human MBP based in part on these new data is presented in an accompanying article (86).

MATERIALS AND METHODS

Purification and Characterization of Bovine MBP/C1—Bovine brain was obtained from 2–4-year-old cattle immediately after death (Ontario Agricultural College). All subsequent manipulations were performed at 4 °C unless otherwise specified. The entire brain was immediately placed in approximately 1 liter of isotonic buffer (145 mM NaCl). The meninges and cortex were carefully removed, and blood was washed away from the remaining tissue with isotonic buffer. The gray matter was removed from the white matter gently using a spatula. This white matter was cut into small pieces approximately 3–5 cm in size and either frozen rapidly and stored at −70 °C until use or used immediately as a source for bovine MBP/C1.

The C1 component of myelin basic protein was isolated essentially as described previously (13, 42). Briefly, a total of approximately 36 g of white matter was homogenized in 4 or 5 small portions in 284 ml of chloroform:methanol (2:1, v:v) for 2 min using a probe sonicator (Pro250, DiaMed Corp., Mississauga, Ontario) at a setting of 4 or 5. This homogenate was stirred overnight at 4 °C and then filtered through Whatman filter paper under gravity at room temperature in the fume hood. The residue remaining on the paper was washed with 130 ml of ice cold chloroform:methanol (2:1, v:v) followed by 172 ml of ice-cold acetone. The residue was then air-dried and was either frozen for up to 2 days at −20 °C before use or immediately resuspended in 130 ml of 100 mM H_2SO_4, 0.1 mM phenylmethylsulfonyl fluoride. The homogenate was gently stirred overnight and centrifuged in a Beckman JA20 rotor at 6,000 × *g* for 1 h. The pellet was resuspended in 52 ml of the same buffer and recentrifuged at 6,000 × *g* for 30 min. The acid-soluble proteins in the pooled supernatants were precipitated by adding an equal volume of ice-cold absolute ethanol and leaving the mixture overnight at −20 °C.

The precipitated protein was recovered by centrifugation at 6,000 × *g* for 1 h at −10 °C. The precipitate was washed twice in 150 ml of 90% ethanol at −20 °C and recovered by centrifugation at 6,000 × *g* for 30 min at −10 °C. The final protein pellet was resuspended in 10 ml of buffer 1 (80 mM glycine, 6 M urea, pH 9.5) and dialyzed overnight against 500 ml of buffer 1 at room temperature. Insoluble material was removed by centrifugation at 6000 × *g* for 15 min at 4 °C. The pH of the supernatant was adjusted to 9.5 with NaOH.

An amount of 80–90 (A_{280}) units of sample was loaded at a rate of 0.1 ml/min onto a Whatman CM52 column (35 × 1 cm) that had been preswollen and preequilibrated with buffer 1 at pH 10.5. Chromatography was performed at room temperature (~18–20 °C). After sample loading, the column was washed with 60 ml of buffer 1 at 12 ml/h for 5 h. Bound protein was eluted by 200 ml of buffer 2 (80 mM glycine, 2 M urea, pH 10.5) in a linear gradient of 0–200 mM NaCl at 12 ml/h. The eluate was monitored at 280 nm and collected in 3-ml fractions. Under these conditions, component C1 of MBP eluted last. The C1-containing fractions were dialyzed against either 1 liter of buffer G (80 mM glycine, pH 7.5, with NaOH, 0.75 mM NaN_3) or buffer S (10 mM HEPES, pH 7.5, with NaOH, 150 mM NaCl, 10 mM $CaCl_2$, 0.75 mM NaN_3) at 4 °C for 24 h and then dialyzed further against 1 liter of the same buffer for another 24 h. The protein concentration was estimated via a commercial colorimetric assay using bicinchoninic acid (Pierce) and diluted to a final concentration of 2.5 or 0.25 mg/ml. Aliquots of bovine MBP/C1 were either used immediately or frozen at −20 °C until use.

To confirm the identity of purified bovine MPB/C1 biochemically and immunologically, 12% discontinuous SDS-polyacrylamide gel electrophoresis and Western blot analyses were performed. In brief, protein samples from varied steps of the purification were separated by 12% discontinuous SDS-polyacrylamide gel electrophoresis in duplicate. One of the gels was silver-stained (Fig. 1). Western blotting was performed on the other gel using a commercial kit (Bio-Rad catalog number 170-6412). The second gel was equilibrated in transfer buffer (10 mM CAPS, pH 11.0, with NaOH, 20% methanol) for 30 min, and electroblotted at 170 mA for 1 h in a Bio-Rad Mini-Protean II blotting apparatus onto a nitrocellulose membrane. The CAPS buffer improved the transfer of bovine MBP/C1 (pI ~10.6) considerably compared with other buffers such as HEPES. The unbound sites in the nitrocellulose membrane were blocked using 3% gelatin. The membrane was then probed with rabbit anti-bovine MBP/C1 polyclonal IgG antibody, and the presence of bovine MBP/C1 was detected using the amplified alkaline phosphatase goat anti-rabbit immunoblot assay kit as directed by the manufacturer.

Electron Microscopy of Bovine MBP/C1—Preparation for electron microscopy was performed using refinements of published protocols as follows. A 13-μl drop of MBP/C1 was incubated in a Teflon well, and a <1-μl droplet of dehydroabietylamine (89) or lipid mixture (90, 91) was touched to the surface, where it formed a monolayer. After some time in a humid environment, the lipid-protein layer on the surface was removed with a copper grid coated with fenestrated plastic (cellulose acetate butyrate), negatively stained with unbuffered (pH ~4) uranyl formate (92), and air-dried. A number of factors were varied in this process: protein concentration (2.5–0.25 mg/ml), substrate at air-water interface (dehydroabietylamine or mixtures of the following lipids: galactocerebroside, phosphatidylethanolamine, phosphatidylcholine, phosphatidylserine, and monosialoganglioside G_{M1}), incubation temperature (20 or 32 °C), incubation time (0.5, 1, 2, 6, 8, and 12 h), pH of the protein solution (10.5 or 7.5), buffer conditions (concentrations of HEPES-NaOH, glycine, NaCl, $CaCl_2$), and subphase density (with or without 20% glycerol). MBP/C1 at 0.25 mg/ml at 32 °C interacted best with a monolayer formed by a 4:1 (v/v) mixture of phosphatidylserine and monosialoganglioside G_{M1} and is the basis of the results presented here. Imaging was performed in a Philips EM400T at a magnification of × 60,000 using the low dose unit and with the sample kept at liquid nitrogen temperature (−185 °C) in a Gatan cryoholder.

Three-dimensional Reconstruction of Bovine MBP/C1—Image analysis as single particle electron crystallography (87, 88) was performed using the IMAGIC-V program (93), with the exception of angular reconstitution (94) using a quaternion-assisted approach (95). Images were digitized at a resolution of 0.31 nm/object level using an IS-1000 gel scanner (Canberra-Packard, Mississauga, Ontario, Canada) on a dissecting microscope and an EMPIX (Rockwood, Ontario, Canada) uniform intensity light box. Totals of 228 and 3117 (preparations in buffer G and buffer S, respectively) smaller images of size 64 × 64 pixels ("picture elements") and containing a single particle within them were extracted from the larger images. Two-dimensional single particle electron image analysis was performed using standard approaches (93, 96). Successive cycles of alignment with respect to a variety of references (97), correspondence analysis, and hierarchical ascendant classification (98) were used to define homogeneous subsets for two-dimensional averaging. Both populations were analyzed independently. In the case of the smaller population from buffer G, the class averages comprised only small numbers of members, and it was decided to use the individual protein images as projections for three-dimensional reconstruction (99). The larger population from buffer S gave statistically significant classification results, and the class averages were deemed suitable to serve as projections.

In preparation for three-dimensional reconstruction, projection image pretreatment comprised mainly background removal (100). Determination of relative Euler angles of projections within each set was performed using quaternion-based angular reconstitution algorithms (95). Three-dimensional reconstructions using weighted back-projection were then performed (99) and were manipulated (thresholded and rotated) using INSIGHT II (BioSym Inc., Parsippany, NJ) molecular graphics software. To get two independent class averages or reconstructions, the projection sets were randomly halved. The Fourier ring and

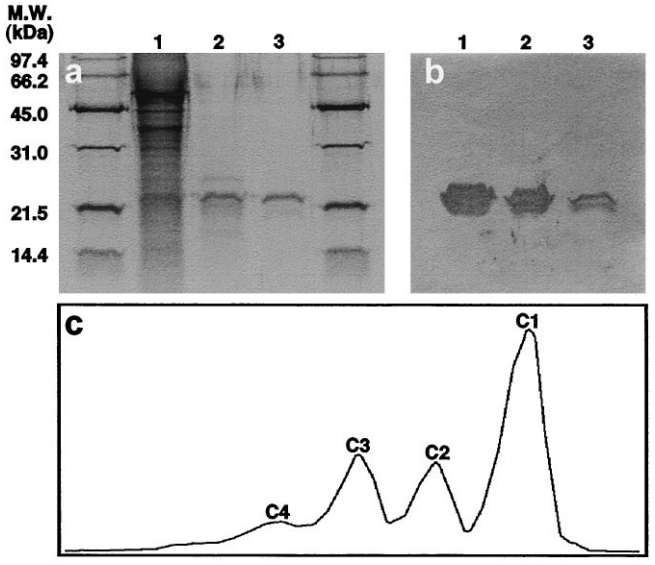

FIG. 1. **Purification and biochemical characterization of myelin basic protein.** *a*, silver-stained polyacrylamide gel of protein from bovine brain. *Lane 1*, bovine brain homogenate; *lane 2*, mixture of all charge isomers of MBP (this sample was loaded onto the CM52 anion exchange column); *lane 3*, purified MBP/C1 charge isomer fraction. All basic proteins (histones, ribosomal proteins, and myelin basic protein) run more slowly in this gel system than predicted by their molecular weights. *b*, Western immunoblot of the polyacrylamide gel in *panel a* using rabbit anti-bovine MBP/C1 IgG. The MBP/C1 charge isomer is present in *lanes 1*, *2*, and *3*. *c*, typical elution profile from a CM52 anion exchange column. The C1, C2, C3, and C4 charge isomers are the ones best separated on this column. For all studies in this paper, the fractions enriched in MBP/C1 were pooled and used.

shell correlation functions were used to estimate the reproducible spatial resolution between two independent two-dimensional averages or three-dimensional reconstructions, respectively (101).

RESULTS

Isolation and Electron Microscopy of Bovine MBP/C1—To obtain material for our experiments, we purified charge component C1 of the 18.5-kDa isoform of MBP from fresh bovine brain under conditions that minimized proteolytic degradation (Fig. 1). A bovine source of the protein yields large and fresher quantities of material than human sources, *i.e.* autopsies. The differences between MBP sequences from the two species are small (29, 30), and it would be expected that bovine MBP and human MBP would have very similar structures.

Preparations of bovine MBP for electron microscopy were undertaken primarily using a lipid monolayer approach (90, 91). The best interaction of MBP with the interface substrate was achieved using a mixture of negatively charged phosphatidylserine and monosialoganglioside G_{M1}. By "best," we mean that the MBP adhered to the lipid monolayer, and large numbers of particles could be seen in the TEM (Fig. 2). Under other incubation conditions, few protein molecules could be seen adsorbing to the lipid film. Occasionally, two-dimensional microcrystals could be found, but these diffracted to only 1 order and were not analyzed further (results not shown). There is no underlying carbon support film in the samples in these micrographs; the protein is suspended in negative stain on lipid monolayers supported over holes in a fenestrated plastic film. We found that cooling the sample to liquid nitrogen temperatures in the electron microscope helped preserve these fragile molecule-containing lipid films during image recording. The appearance of the spreads suggested disordered monolayers of MBP, *i.e.* the protein formed essentially planar and not three-dimensional distributions.

In electron micrographs, bovine MBP/C1 in low salt buffer G appears to have a toroidal or "C" shape and a diameter of approximately 11 nm (Fig. 2, *a* and *b*). In higher salt buffer S, the protein has a more compact spheroidal appearance but is of approximately the same size (Fig. 2, *c* and *d*). The homogeneity of appearance (size and degree of staining) of our preparations makes acceptable the application of both established and emerging techniques of single particle electron crystallography (87, 88). The first step in this process is two-dimensional alignment, multivariate statistical analysis, and hierarchical ascendant classification to define characteristic (recurring) projection views (96–98). The second step is determination of the relative orientations of different projections (94, 95) and three-dimensional reconstruction (99).

Two-dimensional Analysis and Three-dimensional Reconstruction of Bovine MBP/C1—The two-dimensional single particle analysis of the small population (228 particles) of bovine MBP/C1 in buffer G yielded class averages (of approximately 10 members each) that mainly appeared to be subtle variations of the basic "C" shape (not shown). The 228 original images of individual protein molecules were considered to be projections of the same three-dimensional structure at different orientations. Two-dimensional single particle analysis of the larger data set (3117 particles) of bovine MBP/C1 in buffer S yielded convergence to a set of statistically significant class averages shown in Fig. 3. This preparation on the whole was much better in terms of yield of particles and definition of their shape than the one in buffer G. The class averages of Fig. 3 were also interpreted to represent projections of the same three-dimensional structure at different orientations.

Both projection sets (228 and 100 images, respectively), were analyzed by the iterative quaternion-assisted angular determination process (95). The distribution of Euler angles on the unit sphere for each set is shown in Fig. 4. The three-dimensional reconstructions of both projection sets, computed using filtered back-projection, are shown in Figs. 5 and 6 from various perspectives. The reconstructions are thresholded first at a density level corresponding to the volume expected from the protein's molecular mass (18.5 kDa) and then at a higher cut-off to accentuate internal detail. The dimensions are an outer radius of 5.5 nm, an inner radius of 3 nm, an overall circumference of 15 nm, and a height of 4.7 nm. For the first data set, almost all orientations depict the "C" shape, indicating a faithful correspondence with the original projection data. The resolution of this three-dimensional reconstruction was determined to be better than 4 nm. The second three-dimensional reconstruction is not as open as the first "C" one but has roughly the same dimensions as the previous one. Resolution estimates for this structure are 1.7 nm for two-dimensional averages and 2.8 nm for two independent three-dimensional reconstructions. (The canonical significance threshold of two standard deviations as suggested by van Heel (101) was used.) Computer graphical representation and manipulation of both reconstructions enabled the superimposition of the two reconstructions and thus show their overall similarity (Figs. 7 and 8).

DISCUSSION

High resolution TEM is a viable technique to determine structures of biological macromolecules and their complexes (87, 88), especially when (like MBP (85)) these do not form three-dimensional crystals of suitable size and order for x-ray diffractometry. We are aware of only one published TEM study of MBP, which suggested that MBP spread from solution and negatively stained appeared to be fibrous and of dimensions 15×1.5 nm (56). The analysis in this work was qualitative and performed under conditions greatly different from our own here (see below). A decade ago, it was reported that MBP polymerized on the surfaces of erythrocytes and that this effect could be

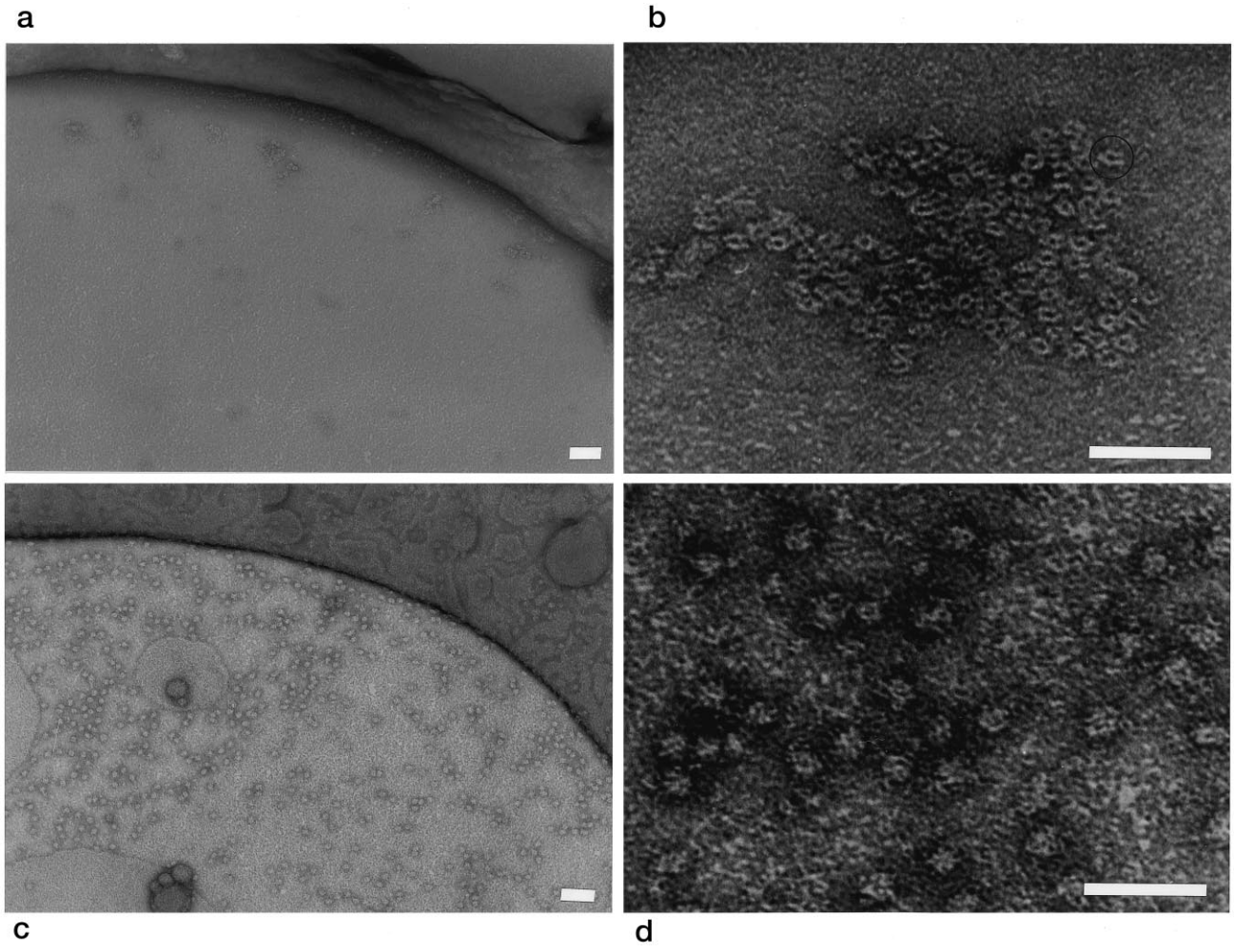

FIG. 2. **Transmission electron micrographs of bovine MBP/C1 particles adhering to a phosphatidylserine:monosialoganglioside G_{M1} monolayer, suspended over a hole in a fenestrated plastic film, negatively contrasted with 2% uranyl formate, and imaged at liquid nitrogen temperature (−185 °C).** *a* and *b*, bovine MBP/C1 in buffer G. In this preparation, an overall "C" shape predominates (*circled*), and the protein tends to cluster together. *c* and *d*, bovine MBP/C1 in buffer S. In this preparation, the protein is dispersed on the monolayer and presents a greater variety of orientations. *Scale bars*, 50 nm.

visualized by scanning electron microscopy, but no micrographs were presented (66). Since MBP is a peripheral membrane protein within the myelin sheath, it was reasonable to hypothesize that it would interact with and then be visualized on lipid monolayers formed at the air-water interface and potentially even form ordered arrays (90, 91). Although we did not achieve the goal of large, two-dimensional crystals, we could analyze using other approaches the images of large numbers of bovine MBP/C1 particles adhering to the lipid monolayer. The best interaction of MBP with the interface substrate was achieved using a mixture of negatively charged phosphatidylserine and monosialoganglioside G_{M1}.

Our results are consistent with previous biochemical data in many respects. It has long been known that MBP can interact strongly with and aggregate acidic lipid vesicles *in vitro* and that the lipid reforms into stable multilamellar layers that resemble *in vivo* myelin as determined by x-ray diffraction and NMR studies (10, 13, 16–21, 23, 24). The attraction between MBP and lipids has been shown by physicochemical, NMR, and Fourier transform infrared spectroscopic studies to be primarily electrostatic with a hydrophobic component whose magnitude and even existence are still debated (9–28). The strongest interaction is with lipids such as cerobroside sulfate or gangliosides (9, 12, 14, 15, 18–20). Thus, it is not surprising that positively charged MBP interacted with negatively charged lipid monolayers and could be visualized by transmission electron microscopy.

MBP also has a marked tendency to self-associate, an effect suggested to be due to hydrophobic interactions (5, 65, 66, 69–71). It also interacts with other proteins such as proteolipid protein (67, 68), calmodulin (12), actin (51), and tubulin (52) and sequesters zinc (72). Thus, it is not unexpected that MBP forms extensive clusters on negatively charged lipid monolayers, especially in the low salt buffer G (Fig. 3*a*). Finally, although MBP in solution is probably fully disordered (5, 55–59), CD and other analyses show that the degree of secondary structure, primarily the amount of α-helix but also β-sheet, increases substantially after phosphorylation and in the presence of organic solvents, detergents, and lipids (59–64). It can be argued that the conformation of bovine MBP/C1 that is formed on lipid monolayers, and that we have visualized, is a biologically more relevant form than isolated protein spread on a hydrophobic carbon film, for example (56). At present, the protein is far too small to be visualized effectively in vitreous ice.

The two-dimensional single particle analysis of the small population (228 particles) of bovine MBP/C1 in buffer G yielded class averages (of approximately 10 members each) that mainly appeared to be subtle variations of the basic "C" shape (not shown). We interpreted this result to mean that the particles

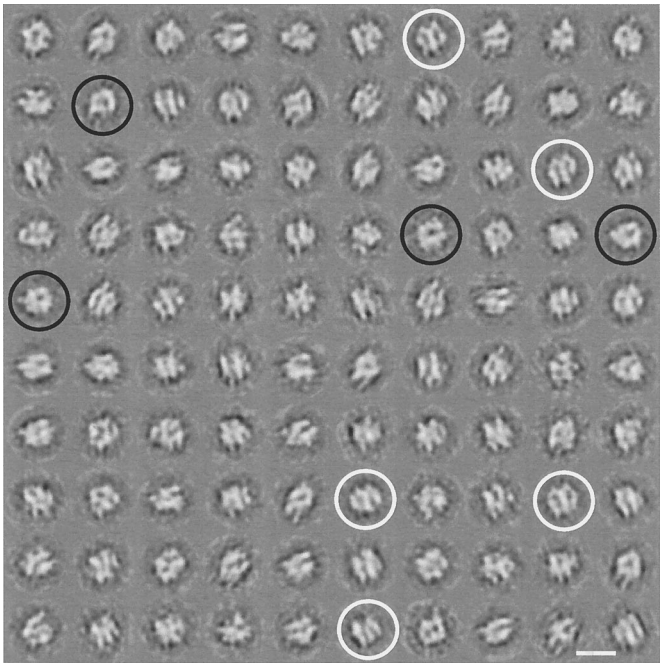

FIG. 3. **Gallery of 100 averages of MBP image classes derived from two-dimensional single particle analysis of 3117 bovine MBP/C1 molecules in buffer S (Fig. 2, *c* and *d*).** We indicate two characteristic views, interpreted to be an "end-on C" (*black circles*) and a "side-on M" (*white circles*). The former projections correspond best to the "C" view seen in low salt buffer G (Fig. 2*a*). In these images, *white* corresponds to protein. *Scale bar*, 10 nm.

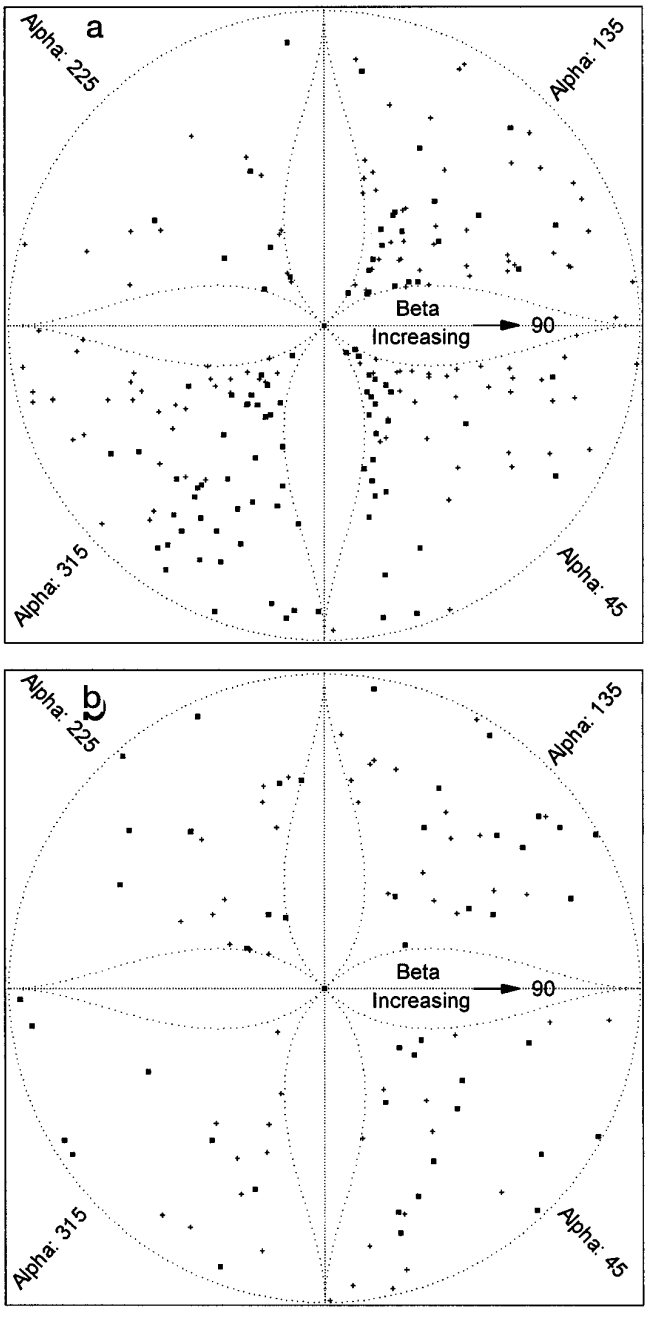

FIG. 4. **The angular orientations of 228 single particles in buffer G (*a*), and 100 class averages of 3117 particles in buffer S (*b*), are plotted here cartographically as points on a spherical surface.** The *square points* represent angular orientations on the foreground hemisphere, and *crosses* show angular orientations on the background hemisphere. The iterative quaternion-assisted angle determination process was used to determine these relative angular orientations of projections of MBP molecules in order to enable a three-dimensional reconstruction. In buffer G, the particles had a tendency to adhere to the lipid monolayer in a "C" orientation (Fig. 2, *a* and *b*). In buffer S, the particles had a wider variety of orientations. Here in *panel b*, the Euler angles are distributed more isotropically than in *panel a*, confirming the visual interpretation.

"wobbled" around this basic projection direction. Because these class averages were not statistically significant, they were not considered further. We decided to use the individual images as projections for three-dimensional reconstruction. Two-dimensional single particle analysis of the larger data set (3117 particles) of bovine MBP/C1 in buffer S yielded convergence to a set of statistically significant class averages shown in Fig. 4, which were used as two-dimensional projections for three-dimensional reconstruction. This preparation on the whole was much better in terms of yield of particles and definition of their shape than the one in buffer G. However, the two populations must be presented together because the preparative conditions in buffer G provide a conceptual link to the putative fibrous conformation of MBP in aqueous solution (56) and were essential in defining a topology of β-strand arrangement in the molecular models of MBP that we have built (86).

The conditions of EM preparation are favorable for generating many orientations of MBP. The protein has a large number of positively charged residues distributed throughout its structure, each of which can interact with the negatively charged monosialoganglioside G_{M1} or phosphatidylserine head groups; and the lipid monolayer is mechanically more flexible than even a thin carbon film and could partially wrap around and cradle each molecule. Also, the results of the two-dimensional electron image analyses indicate that the sets of individual images of MBP molecules should be interpreted as representing *randomly oriented* projections of the same three-dimensional structure. Other situations have been described where such isotropic orientations were achieved, especially using methylamine tungstate as a negative stain (92, 102).

Both pretreated projection sets (228 images and 100 class averages, respectively), were subjected to an iterative quaternion-assisted angular determination process (Fig. 5) (94, 95). This approach has recently been applied to the signal sequence-binding protein (103), nucleosomes (104, 105), ribosomal subunits (100), and other protein complexes. These successful previous endeavors provide confidence in our further application of this algorithm to the randomly oriented projections of the present data. The distribution of Euler angles on the unit sphere for each set is shown in Fig. 5. As suggested from considerations of the class averages, the preparation in buffer S is seen visually to have a more isotropic orientational distribution than the one from buffer G.

The three-dimensional reconstructions of both preparations

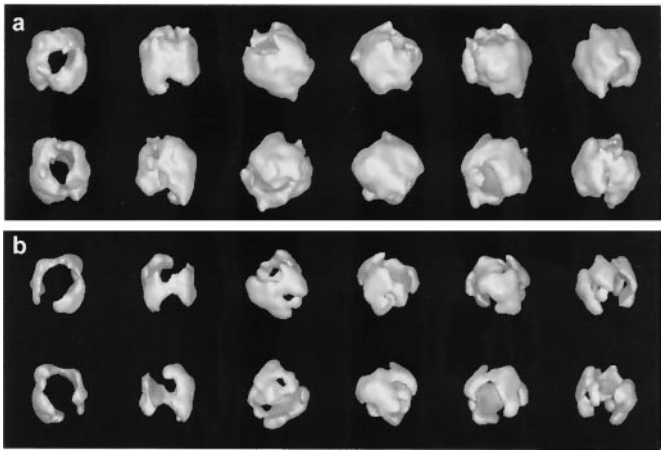

FIG. 5. **Shaded surface views of the three-dimensional reconstruction of 228 projections of bovine MBP/C1 in buffer G are shown from 20 different perspectives.** The three-dimensional volume is thresholded here to a volume comprising the molecular mass (18.5 kDa) of the protein (*a*), and thresholded at a higher density to show more internal detail (*b*).

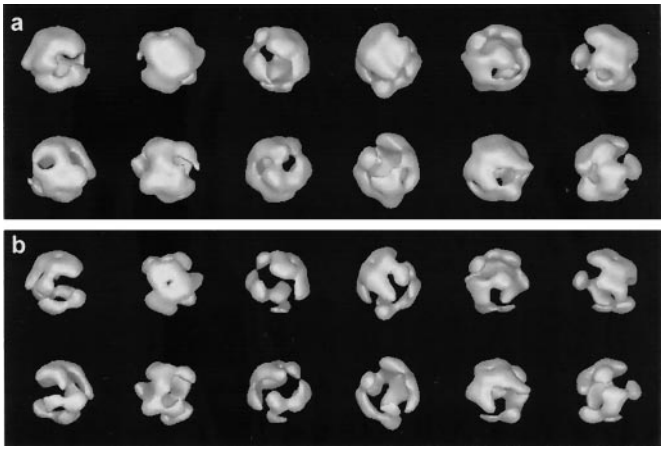

FIG. 6. **Shaded surface views of the three-dimensional reconstruction of 100 projections (class averages from 3117 images of individual proteins) of bovine MBP/C1 in buffer S are shown from 20 different perspectives.** The three-dimensional volume is thresholded here to a volume comprising the molecular mass (18.5 kDa) of the protein (*a*), and thresholded at a higher density to show more internal detail (*b*).

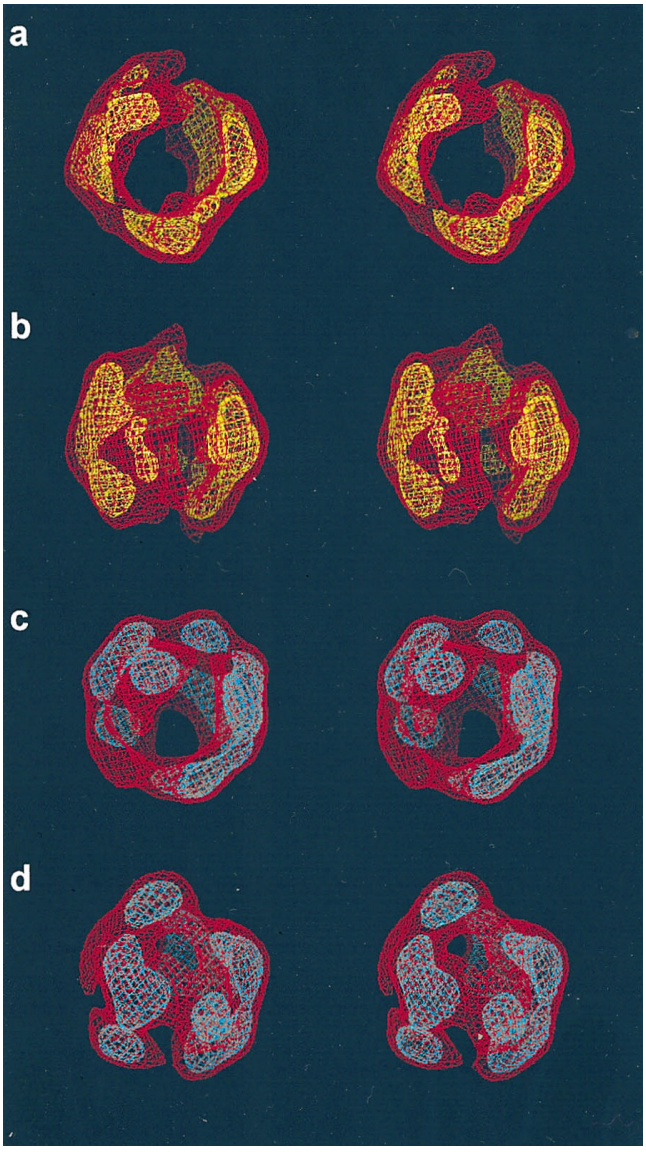

FIG. 7. **Stereo pair images of wire mesh representations of reconstructions of bovine MBP/C1 in buffer G (*a* and *b*), and buffer S (*c* and *d*).** The *red mesh* represents a density cut-off of the reconstruction corresponding to the molecular mass (18.5 kDa) of the protein. The *yellow* and *blue meshes* represent higher density thresholds to illustrate the internal mass distribution. The reconstructions are presented in the top "C" orientation (*a* and *c*) and in the side "M" orientation (*b* and *d*). The "C" view is interpreted to be along a direction perpendicular to the lipid monolayer, while the "M" view is interpreted to be along a direction parallel to the lipid monolayer.

are shown separately in Figs. 5 and 6 and shown together for comparison in Figs. 7 and 8. For the first data set of proteins in buffer G, almost all orientations depict the "C" shape, indicating a faithful correspondence with the original projection data. The dimensions are an outer radius of 5.5 nm, an inner radius of 3 nm, an overall circumference of 15 nm, and a height of 4.7 nm. Epand *et al.* (56) proposed that MBP was a fibrous protein of dimensions 15 × 1.5 nm, but these workers had imaged a mixture of *all* charge isomers (C1 to C8) in aqueous solution; no lipids were present. Thus, the conditions of preparation for EM here are significantly different from those of this earlier work. Nonetheless, the overall length and thickness correspond for the two results, consistent with the idea that the conditions affect the conformation of this protein. If the "C" shape of circumference 15 nm opened up in aqueous solution, then a 15-nm-long rod would be seen. The second three-dimensional reconstruction of proteins in calcium-containing buffer S is not as open as the first "C" one but has roughly the same dimensions. Clearly, the effect of monovalent and divalent cations was to force the structure to close up somewhat. We do not have an explanation for this phenomenon, other than that it might reflect a charge-shielding effect.

These reconstructions of bovine MBP/C1 have several implications for the packing of myelin. The thickness of the major dense line in the myelin sheath is roughly 1.7 nm, and that of the intraperiod line is 2.5 nm. A lipid bilayer is at least about 4.5 nm thick. The charge isomer MBP/C1 is located primarily in the major dense line, while MBP/C8 is located primarily in the intraperiod line (47, 48). Biologically relevant questions that arise are (i) "How does the C1 isomer sit in the major dense line?" and (ii) "How does a conversion to C8 allow a migration through the bilayer into the intraperiod line?" The first question is perhaps the easier one, but the answer is still not clear. The "C" shape of the molecule is surmised to lie flat on the myelin membrane, because this view is seen preferentially in the images of the flat lipid monolayer (not fixed, but rocking about it); in other words, looking perpendicular to the myelin

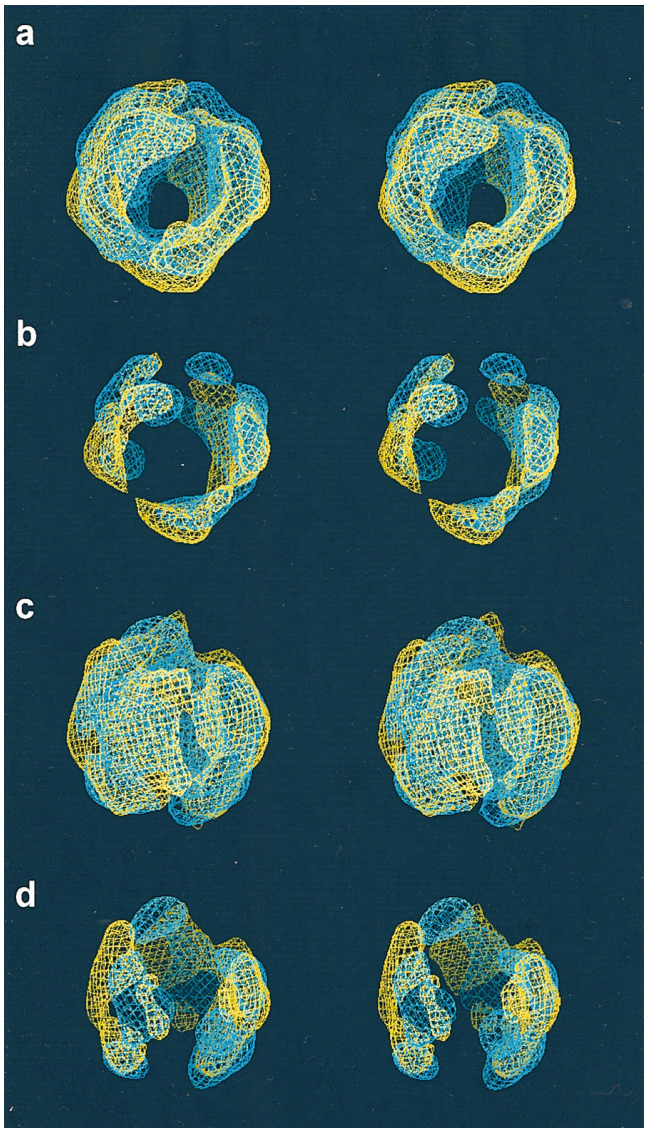

FIG. 8. **Stereo pair images of wire mesh representations of reconstructions of bovine MBP/C1 in buffer G (*yellow*) and buffer S (*blue*).** The reconstructions are superimposed on one another to illustrate the subtle compaction of the protein upon exposure to monovalent and divalent cations. The reconstructions are presented in the top "C" orientation (*a* and *b*), and in the side "M" orientation (*c* and *d*). In *panels a* and *c*, the density thresholds are chosen to correspond to the molecular mass of the protein. In *panels b* and *d*, a higher threshold was applied as in Fig. 7. In the presence of salts, the protein tends to tighten up, whereby the "C" closes up to an "O", and the top of the "M" folds in upon itself to form a cup-like shape.

membrane would mean looking through the cavity (Fig. 2). The joining of two membranes by a single molecule of MBP/C1, of height 4.7 nm would mean the molecule would have to penetrate deeply into apposing bilayers. Clearly, such a scenario represents a forced and tight fit. However, myelin may not necessarily form on preexisting lipid bilayers being laid down initially. Myelin basic protein could be the starting foundation around which lipid is laid, an idea given credence by the observation already made by Napolitano *et al.* (22) that myelin retains a lamellar structure in the *absence* of lipids. It is essential to pursue higher resolution structural analyses of MBP under varied conditions to clarify such issues.

CONCLUSIONS

Myelin basic protein is an unusual protein in many respects. It is flagrantly microheterogeneous in its multitude of isoforms and isomers, and it is the only myelin-associated protein that is absolutely essential for the maintenance of the myelin sheath. Here, we have studied MBP structure by transmission electron microscopy and three-dimensional reconstruction of single particles on lipid monolayers. These data served as constraints for a predicted atomic structure presented in the accompanying paper (86). Our results are consistent with the protein having an overall "C" shape of outer dimension 11 nm, under low salt conditions, and with the protein closing up into a more globular shape in the presence of salt.

Acknowledgments—We are grateful to Dr. Terry Beveridge and Robert Harris (Department of Microbiology, University of Guelph), for access to and assistance with the Philips EM400T and the Gatan cryoelectron microscopic accessories. Dr. Marin van Heel (Imperial College, London) and Dr. Michael Schatz (Image Science GmbH, Berlin) provided access to the IMAGIC-V software package. Dr. Denise Wood and Teresa Miani (Biochemistry Research, Hospital for Sick Children) provided superb tutelage in MBP purification. Drs. Kazuhiro Aoyama, Harald Engelhardt, and especially Tschangiz Scheybani (Max-Planck-Institut für Biochemie, Martinsried, Germany) gave excellent guidance in two-dimensional protein crystallization.

REFERENCES

1. Deber, C. M. & Reynolds, S. J. (1991) *Clin. Biochem.* **24,** 113–134
2. Kirschner, D. A., Inouye, H., Ganser, A. L. & Mann, V. (1989) *J. Neurochem.* **53,** 1599–1609
3. Mateu, L., Luzzati, V., Vonasek, E., Borgo, M. & Lachapelle, F. (1996) *J. Mol. Biol.* **256,** 319–329
4. Moscarello, M. A. (1996) in *Cell Biology and Pathology of Myelin: Evolving Biological Concepts and Therapeutic Approaches* (Devon, R. M., Doucette, R., Juurlink, B. H. J., Nazarali, A. J., Schreyer, D. J. & Verge, V. M. K.) Plenum Press, New York
5. Smith, R. (1992) *J. Neurochem.* **59,** 1589–1608
6. Brady, G. W., Murthy, N. S., Fein, D. B., Wood, D. D. & Moscarello, M. A. (1981) *Biophys. J.* **34,** 345–350
7. Moscarello, M. A., Brady, G. W., Fein, D. B., Wood, D. D., Cruz, T. F. (1986) *J. Neurosci. Res.* **15,** 87–99
8. Staugaitis, S. M., Colman, D. R. & Pedraza, L. (1996) *BioEssays* **18,** 13–18
9. Bach, D. & Sela, B. (1985) *Biochim. Biophys. Acta* **819,** 225–230
10. Boggs, J. M., Moscarello, M. A. & Papahadjopoulos, D. (1977) *Biochemistry* **16,** 5420–5426
11. Boggs, J. M., Wood, D. D. & Moscarello, M. A. (1981) *Biochemistry* **20,** 1065–1073
12. Chan, K.-F. J., Robb, N. D. & Chen, W. H. (1990) *J. Neurosci. Res.* **25,** 535–544
13. Cheifetz, S. & Moscarello, M. A. (1985) *Biochemistry* **24,** 1909–1914
14. Demel, R. A., London, Y., Guerts van Kessel, W. S. M., Vossenberg, F. G. A. & van Deenen, L. L. M. (1973) *Biochim. Biophys. Acta* **311,** 507–519
15. Fidelio, G. D., Maggio, B. & Cumar, F. A. (1982) *Biochem. J.* **203,** 717–725
16. Fraser, P. E., Rand, R. P. & Deber, C. M. (1989) *Biochim. Biophys. Acta* **983,** 23–29
17. Lampe, P. D. & Nelsestuen, G. L. (1982) *Biochim. Biophys. Acta* **693,** 320–325
18. MacNaughtan, W., Snook, K. A., Caspi, E. & Franks, N. P. (1985) *Biochim. Biophys. Acta* **818,** 132–148
19. Maggio, B. & Yu, R. K. (1989) *Chem. Phys. Lipids* **51,** 127–136
20. Maggio, B. & Yu, R. K. (1992) *Biochim. Biophys. Acta* **1112,** 105–114
21. Monferran, C. G., Maggio, B. & Cumar, F. A. (1986) *Mol. Cell. Biochem.* **70,** 131–139
22. Napolitano, L., Lebaron, F. & Scaletti, J. (1967) *J. Cell Biol.* **34,** 817–826
23. Nezil, F. A., Bayerl, S. & Bloom, M. (1992) *Biophys. J.* **61,** 1413–1426
24. Páli, T., Ebert, B. & Horváth, L. I. (1987) *Biochim. Biophys. Acta* **904,** 346–352
25. Pérez-Gil, J. & Keough, K. M. W. (1994) *J. Theor. Biol.* **169,** 221–229
26. Reinl, H. M. & Bayerl, T. M. (1993) *Biochim. Biophys. Acta* **1151,** 127–136
27. Surewicz, W. K., Moscarello, M. A. & Mantsch, H. H. (1987) *Biochemistry* **26,** 3881–3886
28. ter Beest, M. B. A. & Hoekstra, D. (1993) *Eur. J. Biochem.* **211,** 689–696
29. Carnegie, P. R. (1971) *Biochem. J.* **123,** 57–67
30. Eylar, E. H., Brostoff, S., Hashim, G., Caccam, J. & Burnett, P. (1971) *J. Biol. Chem.* **246,** 5770–5784
31. Kies, M. (1965) *Annu. N. Y. Acad. Sci.* **122,** 161–170
32. Campagnoni, A. T. (1988) *J. Neurochem.* **51,** 1–14
33. de Ferra, F., Engh, H., Hudson, L., Kamholz, J., Puckett, C., Molineaux, S. & Lazzarini, R. A. (1985) *Cell* **43,** 721–727
34. Saavedra, R. A., Fors, L., Aebersold, R. H., Arden, B., Horváth, S., Sanders, J. & Hood, L. (1989) *J. Mol. Evol.* **29,** 149–156
35. Erickson, A. K., Payne, D. M., Martino, P. A., Rossomondo, A. J., Shabanowitz, J., Weber, M. J., Hunt, D. F. & Sturgill, T. W. (1990) *J. Biol. Chem.* **265,** 19728–19735
36. Deibler, G. E., Stone, A. L. & Kies, M. W. (1990) *Proteins Struct. Funct. Genet.* **7,** 32–40
37. Ramwani, J. J., Epand, R. M. & Moscarello, M. A. (1989) *Biochemistry* **28,** 6538–6543
38. Ulmer, J. B. (1988) *Prog. Neurobiol.* **31,** 241–259
39. Chan, C. K., Ramwani, J. & Moscarello, M. A. (1987) *Biochem. Biophys. Res. Commun.* **152,** 1468–1473
40. Chou, F. C.-H., Chou, C.-H. J., Shapira, R. & Kibler, R. F. (1976) *J. Biol. Chem.* **251,** 2671–2679

41. Moscarello, M. A., Pang, H., Pace-Asciak, C. R. & Wood, D. D. (1992) *J. Biol. Chem.* **267,** 9779–9782
42. Wood, D. D. & Moscarello, M. A. (1989) *J. Biol. Chem.* **264,** 5121–5127
43. Wood, D. D. & Moscarello, M. A. (1996) in *The Molecular Biology of Multiple Sclerosis* (Russell, W., ed) John Wiley & Sons, Inc., New York
44. Moscarello, M. A., Wood, D. D., Ackerley, C. & Boulias, C. (1994) *J. Clin. Invest.* **94,** 146–154
45. Wood, D. D., Bilbao, J. M., O'Connors, P. & Moscarello, M. A. (1996) *Ann. Neurol.* **40,** 18–24
46. Brunner, C., Lassmann, H., Waehneldt, T. V., Matthieu, J.-M. & Linington, C. (1989) *J. Neurochem.* **52,** 296–304
47. McLaurin, J., Hashim, G. & Moscarello, M. A. (1992) *J. Neurochem.* **59,** 1414–1420
48. McLaurin, J., Ackerley, C. A. & Moscarello, M. A. (1993) *J. Neurochem. Res.* **35,** 618–628
49. Tompkins, T. A. & Moscarello, M. A. (1993) *Arch. Biochem. Biophys.* **302,** 476–483
50. Tompkins, T. A. & Moscarello, M. A. (1994) *Biochim. Biophys. Acta* **1206,** 208–214
51. Dobrowolski, Z., Osinska, H., Mossakowska, M. & Barylko, B. (1986) *Eur. J. Cell Biol.* **42,** 17–26
52. Pirollet, F., Derancourt, J., Haiech, J., Job, D. & Margolis, R. L. (1992) *Biochemistry* **31,** 8849–8855
53. Mastronardi, F. G., Ackerley, C. A., Arsenault, A. L., Roots, B. I. & Moscarello, M. A. (1993) *J. Neurosci. Res.* **36,** 315–324
54. Vanguri, P., Lee, E., Henkart, P. & Shin, M. L. (1993) *J. Immunol.* **150,** 2431–2439
55. Chapman, B. E. & Moore, W. J. (1976) *Biochem. Biophys. Res. Commun.* **73,** 758–766
56. Epand, R. M., Moscarello, M. A., Zierenberg, B. & Vail, W. J. (1974) *Biochemistry* **13,** 1264–1267
57. Gow, A. & Smith, R. (1989) *Biochem. J.* **257,** 535–540
58. Krigbaum, W. R. & Hsu, T. S. (1975) *Biochemistry* **14,** 2542–2546
59. Stuart, B. H. (1996) *Biochem. Mol. Biol. Int.* **38,** 839–845
60. Anthony, J. S. & Moscarello, M. A. (1971) *Biochim. Biophys. Acta* **243,** 429–433
61. Keniry, M. A. & Smith, R. (1979) *Biochim. Biophys. Acta* **578,** 381–391
62. Keniry, M. A. & Smith, R. (1981) *Biochim. Biophys. Acta* **668,** 107–118
63. Mendz, G. L. & Moore, W. J. (1982) *Biochem. Biophys. Res. Commun.* **105,** 1333–1340
64. Smith, R. (1977) *Biochim. Biophys. Acta* **491,** 581–590
65. Afshar-Rad, T., Bailey, A. I., Luckham, P. F., MacNaughtan, W. & Chapman, D. (1987) *Biochim. Biophys. Acta* **915,** 101–111
66. Bellini, T., Rippa, M., Matteuzi, M., Paolino, E. & Dallochio, F. (1987) *Ital. J. Biochem.* **35,** 131A–132A
67. Edwards, A. M., Ross, N. W., Ulmer, J. B. & Braun, P. E. (1989) *J. Neurosci. Res.* **22,** 97–102
68. Golds, E. E. & Braun, P. E. (1978) *J. Biol. Chem.* **253,** 8162–8170
69. Moskaitis, J. E., Shriver, L. C., Campagnoni, A. T. (1987) *Neurochem. Res.* **12,** 409–417
70. Smith, R. (1980) *Biochemistry* **19,** 1826–1831
71. Smith, R. (1982) *Biochemistry* **21,** 2697–2701
72. Cavatorta, P., Giovanelli, S., Bobba, A., Riccio, P., Szabo, A. G. & Quagliariello, E. (1994) *Biophys. J.* **66,** 1174–1179
73. Inouye, H. & Kirschner, D. A. (1984) *Biochim. Biophys. Acta* **776,** 197–208
74. Fraser, P. E. & Deber, C. M. (1985) *Biochemistry* **24,** 4593–4598
75. Koshy, K. M., Hashim, G. A. & Boggs, J. M. (1996) *Biochim. Biophys. Acta* **1293,** 23–30
76. Mendz, G. L., Barden, J. A. & Martenson, R. E. (1995) *Eur. J. Biochem.* **231,** 659–666
77. Mendz, G. L. & Moore, W. J. (1985) *Biochem. J.* **229,** 305–313
78. Price, W. S., Mendz, G. L. & Martenson, R. E. (1988) *Biochemistry* **27,** 8990–8999
79. Golubovich, V. P., Kirnaskh, L. I. & Galaktionov, S. G. (1989) *Biophysics* **34,** 395–399
80. Inouye, H. & Kirschner, D. A. (1991) *J. Neurosci. Res.* **28,** 1–17
81. Martenson, R. E. (1981) *J. Neurochem.* **36,** 1543–1560
82. Martenson, R. E. (1986) *J. Neurochem.* **46,** 1612–1622
83. Stoner, G. L. (1984) *J. Neurochem.* **43,** 433–447
84. Stoner, G. L. (1990) *J. Neurochem.* **55,** 1404–1411
85. Sędzik, J. & Kirschner, D. A. (1992) *Neurochem. Res.* **17,** 157–166
86. Ridsdale, R. A., Beniac, D. R., Tompkins, T. A., Moscarello, M. A., and Harauz, G. (1997) *J. Biol. Chem.* **272,** 4269–4275
87. Frank, J. (1996) *Three-dimensional Electron Microscopy of Macromolecular Assemblies*, p. 104, Academic Press, Inc., New York
88. Yada, R. Y., Harauz, G., Marcone, M. F., Beniac, D. R. & Ottensmeyer, F. P. (1995) *Trends Food Sci. Technol.* **6,** 265–270
89. Aoyama, K., Ogawa, K., Kimura, Y. & Fujiyoshi, Y. (1995) *Ultramicroscopy* **57,** 345–354
90. Jap, B. K., Zulauf, M., Scheybani, T., Hefti, A., Baumeister, W., Aebi, U. & Engel, A. (1992) *Ultramicroscopy* **46,** 45–84
91. Scheybani, T., Baumeister, W., Yoshimura, H. & Nagayama, K. (1994) *Supramolecular Sci.* **1,** 111–116
92. Bremer, A., Henn, C., Engel, A., Baumeister, W. & Aebi, U. (1992) *Ultramicroscopy* **46,** 85–111
93. van Heel, M., Harauz, G., Orlova, E. V., Schmidt, R. & Schatz, M. (1996) *J. Struct. Biol.* **116,** 17–24
94. van Heel, M. (1987) *Ultramicroscopy* **21,** 111–124
95. Farrow, N. A. & Ottensmeyer, F. P. (1992) *J. Opt. Soc. Am. A* **9,** 1749–1760
96. Frank, J. (1989) *Electron Microsc. Rev.* **2,** 53–74
97. Harauz, G., Boekema, E. J. & van Heel, M. G. (1988) *Methods Enzymol.* **164,** 35–49
98. van Heel, M. (1989) *Optik* **82,** 114–126
99. Harauz, G. & van Heel, M. G. (1986) *Optik* **73,** 146–156
100. Beniac, D. R., Czarnota, G. J., Bartlett, T. A., Rutherford, B. L., Ottensmeyer, F. P. & Harauz, G. (1996) *Scanning Microsc. Suppl.* **11,** in press
101. van Heel, M. (1987) *Ultramicroscopy* **21,** 95–100
102. Stoops, J. K., Baker, T. S., Schroeter, J. P., Kolodziej, S. J., Niu, X.-D. & Reed, L. J. (1992) *J. Biol. Chem.* **267,** 24769–24775
103. Czarnota, G. J., Andrews, D. W., Farrow, N. A. & Ottensmeyer, F. P. (1994) *J. Struct. Biol.* **113,** 35–46
104. Bazett-Jones, D. P., Mendez, E., Czarnota, G. J., Ottensmeyer, F. P. & Allfrey, V. G. (1996) *Nucl. Acids Res.* **24,** 321–329
105. Czarnota, G. J. & Ottensmeyer, F. P. (1996) *J. Biol. Chem.* **271,** 3677–3683